European Journal of Cell Biology 98 (2019) 27–35

Contents lists available at ScienceDirect

European Journal of Cell Biology

journal homepage: www.elsevier.com/locate/ejcb

Research paper

# A novel overlapping NLS/NES region within the PH domain of Rho Guanine Nucleotide Exchange Factor (RGNEF) regulates its nuclear-cytoplasmic localization

Michael V. Tavolieri[a], Cristian A. Droppelmann[b], Danae Campos-Melo[b], Kathryn Volkening[a,b], Michael J. Strong[a,b,*]

[a] Department of Clinical Neurological Sciences, Schulich School of Medicine & Dentistry, Western University, London, Ontario, Canada
[b] Molecular Medicine Group, Robarts Research Institute, Western University, London, Ontario, Canada

ARTICLE INFO

*Keywords:*
Rho Guanine Nucleotide Exchange Factor (RGNEF)
Pleckstrin homology (PH) domain
Nuclear localization
NLS
NES

ABSTRACT

Rho Guanine Nucleotide Exchange Factor (RGNEF) is a 190 kDa protein implicated in both amyotrophic lateral sclerosis (ALS) and cancer. Under normal physiological conditions, RGNEF is predominantly cytoplasmic with moderate levels of nuclear localization. We have identified a 23-amino acid region containing a bipartite nuclear localization signal (NLS) within the Pleckstrin Homology (PH) domain of RGNEF, which when deleted or mutated abolishes the nuclear localization of this protein. Fusion proteins containing only the PH domain demonstrated that this region by itself is able to translocate a 160 kDa protein to the nucleus. Interestingly, we also detected a nuclear export signal (NES) within the linker region of this bipartite NLS which is able to export from the nucleus a fusion protein containing two NLSs. Experiments using Leptomycin-B -an inhibitor of nuclear export- confirmed that this region promotes nuclear export in an exportin-1 dependent manner. This study is the first report demonstrating either of these signals embedded within a PH domain. Notably, this is also the first description of a functional overlapped NLS/NES signal.

## 1. Introduction

Rho guanine nucleotide exchange factor (RGNEF) is a 190 kDa protein that is unique in the human proteome for its ability to act both as a guanine exchange factor (GEF) and an RNA-binding protein which regulates mRNA stability (Droppelmann et al., 2014, 2013; Volkening et al., 2010). Under normal physiological conditions, RGNEF is mainly cytoplasmic and localizes at moderate levels to the nucleus (Droppelmann et al., 2013). RGNEF and its murine homologue p190RhoGEF serve as survival factors in response to oxidative and osmotic stress *in vitro* (Cheung et al., 2017; Wu, 2003) and as a stress response factor *in vivo*, showing significantly upregulated levels following distal sciatic nerve injury in mice (Cheung et al., 2017). RGNEF has been demonstrated to have a relevant role in amyotrophic lateral sclerosis (ALS) forming cytoplasmic inclusions that co-aggregate with other ALS-related proteins in spinal cord motor neurons (Droppelmann et al., 2013; Keller et al., 2012). Additionally, it has been observed that RGNEF plays a role in colon carcinoma through its interaction with focal adhesion kinase (FAK) which facilitates tumor growth and invasion (Yu et al., 2011).

RGNEF has several functional domains, including a Leucine-rich region, a cysteine-rich Zn binding domain, a Dbl homology domain (DH), a Pleckstrin homology domain (PH) and an RNA-binding domain (Droppelmann et al., 2014). PH domains are thought to localize proteins to substrate-rich plasma membranes, though evidence suggests PH domains could also be involved in nuclear localization. Seven of the nine commonly studied PH domain-containing proteins of a molecular weights of 60 kDa or greater have been shown to localize to some extent into the nucleus (Bertagnolo et al., 1998; Kim et al., 1996; Lim et al., 2003; Marmiroli et al., 1994; Nore et al., 2000; Pountney et al., 2008; Stallings et al., 2005; Tang et al., 2003; Yamaga et al., 1999; Ye et al., 2002), though for none of them has a mechanism of nuclear import yet been described.

The maximum molecular weight of proteins that can undergo passive diffusion across the nuclear membrane is a matter of debate, with reports citing 40 kDa (Marfori et al., 2011; Peters, 1984), 60 kDa (Fontes et al., 2000; Gorlich and Mattaj, 1996; Mattaj and Englmeier, 1998), or 110 kDa (Wang and Brattain, 2007). However, beyond the

* Corresponding author at: Rm C7-120, University Hospital, LHSC, 339 Windermere Road, London, Ontario, N6A 5A5, Canada.
*E-mail addresses:* mtavolie@uwo.ca (M.V. Tavolieri), cdroppel@uwo.ca (C.A. Droppelmann), dmaribel@uwo.ca (D. Campos-Melo), kvolkening@robarts.ca (K. Volkening), Michael.Strong@schulich.uwo.ca (M.J. Strong).

https://doi.org/10.1016/j.ejcb.2018.11.001
Received 15 June 2018; Received in revised form 8 October 2018; Accepted 13 November 2018

molecular weight threshold, transport across the nuclear membrane is an active, energy-dependent process performed by specialized proteins termed karyopherins which account for approximately 45% of active transport into the nucleus (classical nuclear import pathway) (Lange et al., 2007). Two karyopherins, importin-α and importin-β, form a heterodimer (Hubner et al., 1997; Kalderon et al., 1984a, b) which then binds a single cargo protein at clusters of basic amino acids within the nuclear localization signal (NLS) and shuttle the bound protein into the nucleus. NLSs are either monopartite, having a single cluster of basic residues, or bipartite, containing two clusters of basic residues separated by a mutation tolerant linker sequence between 9 and 29 amino acid residues in length (Dingwall and Laskey, 1991; Lange et al., 2010). PH domains contain basic residues located on the exterior of β-sandwich sheets which interact with phosphoinositides embedded within membranes (Lemmon and Ferguson, 2000), similar to how basic residues of NLSs interact with importin-α (Dingwall and Laskey, 1991; Lange et al., 2010).

In addition, the most common nuclear export pathway requires interaction between the cargo protein and the karyopherin exportin-1. This interaction is facilitated by a nuclear export signal (NES) (Bogerd et al., 1996) which can be classified in six subclasses (Kosugi et al., 2008b). The analysis based on amino acid consensus sequences is currently used as a starting point for the confirmation of functional NES sequences (Xu et al., 2012). It has been observed that nuclear export rates appear to be largely dependent on the accessibility of the NES rather than strictly on binding affinity (Henderson and Eleftheriou, 2000).

In this study, we have characterized a bipartite NLS embedded within the PH domain of RGNEF that is both necessary and sufficient for its nuclear localization. We have also identified a Leptomycin-B sensitive NES located within the PH domain, overlapping with the NLS. These unique observations suggest that the PH domain of RGNEF may serve a critical role in not only mediating protein localization to the cell surface membrane, but also in regulating RGNEF transport across the nuclear membrane.

## 2. Material and methods

### 2.1. Constructs

The plasmid encoding human RGNEF (pcDNA-RGNEF-myc) was previously generated in our lab (Droppelmann et al., 2013). pcDNA-RGNEF-ΔPH-myc, a deletion construct lacking the PH domain (residues 1083–1201) was generated by standard molecular biology procedures. Site-directed mutagenesis (QuickChange Lightning Multi Site-Directed Mutagenesis Kit; Agilent Technologies) of pcDNA-RGNEF-myc was used to mutate basic residues of the NLS to neutral alanine residues (R1101 A, K1103 A, K1120 A, & K1123 A) and create a myc-tagged NLS-lacking construct pcDNA-RGNEF-mutNLS-myc.

The PH domain of either wild-type RGNEF or of our mutant NLS RGNEF were inserted into either pHM830 or pHM840 vectors (Addgene) resulting in the expression of fusion proteins of 160 kDa.

### 2.2. Cell lines and transfections

HEK293 T and SH-SY5Y cells were maintained in Dulbecco's modified Eagle's medium (Life Technologies) supplemented with 10% fetal bovine serum (Life Technologies). SH-SY5Y cells were treated with 10 μM retinoic acid (Sigma-Aldrich) for 3 days prior to transfection to induce a neuron-like phenotype (Encinas et al., 2000). Transient transfections were performed using Lipofectamine 2000 (Life Technologies) in 6-well plates according to the manufacturer's protocols.

### 2.3. Subcellular fractionation

Nuclear and cytoplasmic fractions were isolated as previously described (Liu and Fagotto, 2011). Briefly, cell membranes were semi-permeabilized by 10 min incubation in 42 μg/ml digitonin (Sigma-Aldrich) dissolved in 1X NEH buffer (150 mM NaCl, 0.2 mM EDTA, 20 mM Hepes-NaOH - pH 7.4). The solution was then collected and stored as "cytoplasmic fraction". Plates were scraped, and the remaining cellular components were collected and homogenized using a Dounce homogenizer. The sample was centrifuged at 1,000 × *g* for 10 min and the supernatant was collected as "nuclear fraction".

### 2.4. Western blot

Protein samples were mixed with loading buffer containing SDS and separated electrophoretically by 10% SDS-PAGE. Proteins were transferred to nitrocellulose membranes and then incubated with primary antibodies for 90 min and after with secondary antibodies for 60 min. Immunoblots were developed using chemiluminescence (Western Lightning Plus ECL; PerkinElmer) and visualized with a Bio-Rad ChemiDoc XRS + system. Primary antibodies were directed against c-myc (1:4000; Cedarlane; cat#CLX229AP), GAPDH (1:2000; Abcam; cat#ab9485), and Lamin A/C (1:500; Santo Cruz; cat#ab68417). Secondary antibodies were HRP conjugated: Goat anti-mouse (1:5000; Bio-Rad; cat#170-6516), Swine anti-rabbit (1:2500; Dako; cat#P039901-2), and Mouse anti-rabbit (1:5000; Santa Cruz; cat#1721011).

### 2.5. GEF activity

The activation of RhoA by RGNEF in HEK293T cells was determined using the "G-LISA Rho Activation Assay Biochem Kit (Luminescence based)" (Cytoskeleton Inc.) according to the manufacturer's instructions. Cells were transfected with pcDNA-RGNEF-myc, pcDNA-RGNEF-mutNLS-myc, and pcDNA3.1-myc-His as control. The activation of RhoA, dependant on RGNEF's GEF activity, was evaluated in basal conditions after 6 h of serum starving.

### 2.6. Immunofluorescence and confocal microscopy

Briefly, coverslips were fixed by incubating for 15 min in 4% paraformaldehyde solution and permeabilized by incubating for 10 min in 0.2% Triton X-100. Coverslips were then incubated in 50 mM ammonium chloride for 30 min to quench aldehyde groups and reduce background staining. Coverslips were blocked with 8% bovine serum albumin (BSA; Fisher Scientific Company) and then incubated with primary antibody for 90 min at room temperature and then incubated for 60 min with secondary antibody. Primary antibodies directed against c-myc (1:250, Cedarlane; cat# CLX229AP) and β III Tubulin (1:60, Sigma-Aldrich; cat# T8578). Secondary antibodies goat anti-mouse Alexa Fluor 488 (1:800, Life Technologies; cat# A11029), and goat anti-rabbit Alexa Fluor 546 (1:800, Life Technologies; cat# A11035) were used. The visualization of the actin cytoskeleton in SH-SY5Y cells was performed in basal conditions after 6 h of serum starving using the "F-actin visualization biochem kit" (Cytoskeleton Inc.). SH-SY5Y cells were used because they form better actin fibers (f-actin) compared to HEK293T cells. Cover slips were incubated in 1 μg/mL Hoechst stain to visualize nuclei. Cover slips were mounted to microscope slides using fluorescent mounting media (Dako). All samples were examined using a Confocal Laser Scanning Platform Microscope (Leica SP8 or Olympus Fluorview 1000 microscopes) and LAS X software (Leica Microsystems Inc.) or FV10-ASW Software (Olympus Corp.).

The percentage of cells showing expression in the nucleus was calculated by counting the number of cells showing nuclear localization and dividing by the total cells expressing the protein (n = 100). Nuclear:cytoplasmic ratios were calculated using intensity profiles generated by LAS X software. The mean intensity within either the nuclear or cytoplasmic compartments was determined and expressed as a ratio.

### 2.7. Statistical analysis

All statistical analyses were done using GraphPad Prism 6. One-way ANOVA with Tukey post-hoc test was performed to determine statistical significance and obtain p values.

### 2.8. In silico analysis

The online service cNLS mapper (http://nls-mapper.iab.keio.ac.jp/cgi-bin/NLS_Mapper_form.cgi) was used to predict the location of putative NLSs. The software predicts NLSs based on the results of a series of activity-based profiles using synthetic NLSs of different affinities (Kosugi et al., 2008a, a; Kosugi et al., 2009b). Molecular modeling was performed using I-Tasser software (http://zhanglab.ccmb.med.umich.edu/I-TASSER/), which predicts protein structure using modeling by iterative threading assembly simulation (Roy et al., 2010; Yang et al., 2015; Zhang, 2008). The models were then visualized using RasTop 2.2 (by Philippe Valadon). We used the online service NetNES 1.1 (http://www.cbs.dtu.dk/services/NetNES/), which identifies putative NES using a machine learning prediction to assess NES scores to residues (la Cour et al., 2004). We used the online service Clustal Omega (http://www.ebi.ac.uk/Tools/msa/clustalo/) - which aligns proteins based on sequence identity - to identify the specific residues responsible for NES activity.

## 3. Results

### 3.1. RGNEF contains a PH domain-embedded NLS

RGNEF contains a Pleckstrin Homology (PH) and Dbl Homology (DH) domain (Droppelmann et al., 2013) (Fig. 1A) in the carboxy terminal half of the protein, which are responsible for RGNEF's GEF activity. In addition to a conserved sequence motif, PH domains are characterized by their distinctive folding: a seven-stranded anti-parallel β-sandwich that is closed at one end by a C-terminal alpha helix (Cozier et al., 2004; Lemmon, 2004). We used I-Tasser software (Roy et al., 2010; Yang et al., 2015; Zhang, 2008) to predict the folding structure of the PH domain of RGNEF from its amino acid sequence. This yielded a seven-stranded anti-parallel β-sandwich with a C-terminal alpha helix consistent with the consensus structure expected for PH domains (Fig. 1B and C). To determine whether the PH domain of RGNEF contained a functional NLS, we analyzed the amino acid sequence of the PH domain using the cNLS Mapper software (Kosugi et al., 2008a; Kosugi et al., 2009a; Kosugi et al., 2009b). This software predicted a bipartite NLS from residues 1100–1127 of the PH domain (Fig. 1B) with the basic residues, expected to interact with importin-α, located either outside of, or towards the edges of, the β-sheets where they would localize to the exterior of the protein and likely be accessible for interaction (Fig. 1C). These data suggest that this region could possibly serve as a functional NLS.

### 3.2. The PH domain-embedded NLS is necessary for RGNEF nuclear localization

To analyze the functionality of this putative NLS signal, we created two mutant constructs of RGNEF: pcDNA-RGNEF-ΔPH-myc which included a deletion of the 119 residues of the PH domain (del 1084–1202) and pcDNA-RGNEF-mutNLS-myc in which four basic residues of the putative NLS were point-mutated to neutral alanine residues (R1101 A, K1103 A, K1120 A, and K1123 A) without inducing major changes in the predicted folding of the protein (Fig. 2A and Fig S1A). HEK293 T cells transfected with the vector expressing wild-type (wt) RGNEF (pcDNA-RGNEF-myc) showed predominantly cytoplasmic localization of the protein with moderate levels of nuclear localization (Fig. 2B), consistent with what we observed previously (Droppelmann et al., 2013). Both NLS lacking constructs showed protein largely absent from the nucleus (Fig. 2B).

To quantify the difference in cellular localization between constructs, we analyzed the distribution of the proteins in transfected cells using intensity profiles generated by LAS X software (Fig S1B) and determined the percentage of construct expressing cells that showed protein localized to the nucleus. Cells transfected with either mutant construct had a significantly lower percentage of cells showing nuclear localization than those expressing RGNEF-wt (RGNEF-ΔPH, $p < 0.0001$; RGNEF-mutNLS $p = 0.0001$) (Fig. 2C). We further quantified differences in nuclear localization using subcellular fractionation and western blot. A statistically significant difference was observed in nuclear fractions in which cells expressing RGNEF-wt show significantly greater nuclear levels of protein than observed for either of the two mutants (RGNEF-ΔPH, $p = 0.0354$; RGNEF-mutNLS $p = 0.0373$, Fig. 2D and E) in which the NLS was deleted or point-mutated.

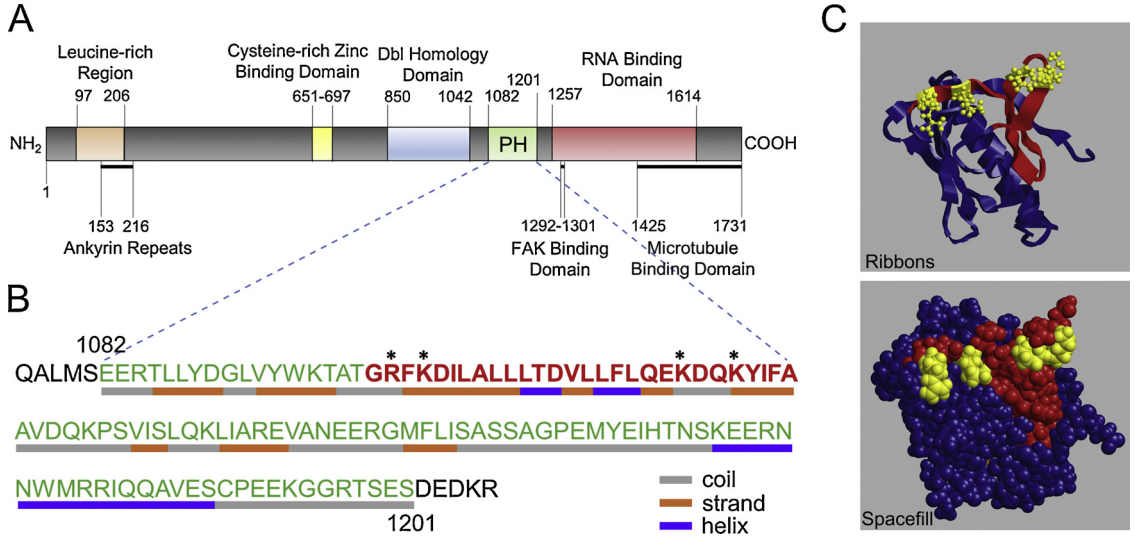


**Fig. 1.** Schematic of the PH domain of RGNEF. (A) Schematic representation of the domains of RGNEF. (B) Amino acid sequence of the PH domain of RGNEF. The nuclear localization signal (NLS) is shown in red with the basic residues marked with asterisks. Grey, orange, and blue underline show the structural prediction and represent coil, β-Strand, and α-Helix, respectively. (C) Ribbon and spacefill models of the PH domain of RGNEF. The NLS is shown in red with the basic residues colored in yellow.

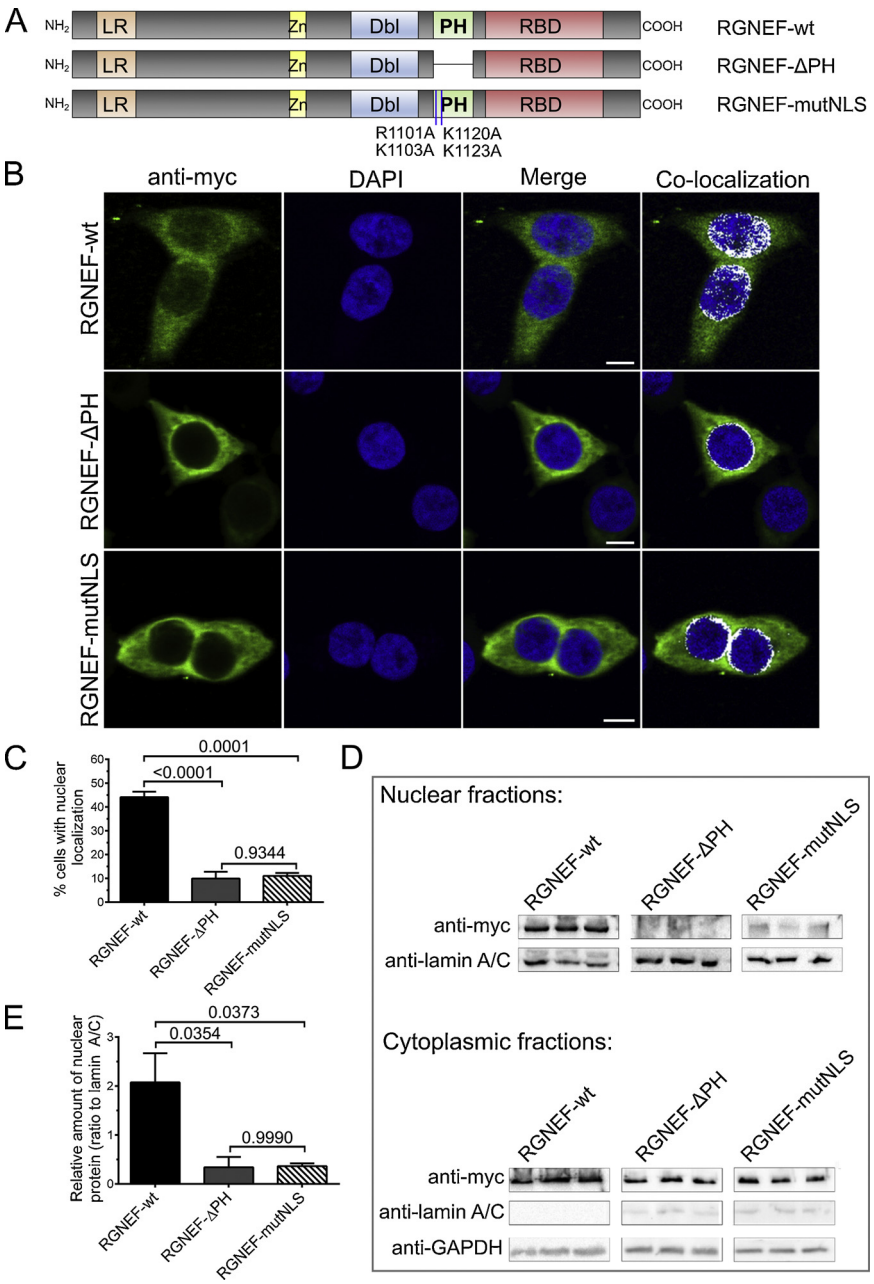


**Fig. 2.** The NLS in the PH domain of RGNEF is essential for its nuclear localization. (A) Schematic representation of the three RGNEF constructs used in subcellular localization experiments. (B) Representative confocal images of HEK293T cells transfected with myc-tagged RGNEF-wt or the mutant constructs, which both lacking a functional NLS. Cells transfected with RGNEF-wt show moderate levels of nuclear localization, where as those transfected with RGNEF-ΔPH or RGNEF-mutNLS fail to show RGNEF within the nucleus. White indicates co-localized pixels. Scale bar = 15 μm. (C) Quantification of cellular localization of confocal images in B. Both RGNEF-ΔPH and RGNEF-mutNLS showed significantly lower levels of cells showing nuclear localization than RGNEF-wt. Means were compared by ANOVA using Tukey's post-hoc test and p values are indicated. Graph shows means ± SEM. (D) Western blot performed using HEK293T cells lysates transfected with myc-tagged RGNEF constructs and separated by subcellular fractionation. α-Lamin A/C (exclusively nuclear) and α-GAPDH are used as loading controls. (E) Densitometry analysis of experiment showed in D. Nuclear fractions from cells transfected with either mutant RGNEF construct showed lower levels of protein than those expressing RGNEF-wt. Means compared by ANOVA using Tukey's post-hoc test and p values are indicated. Graph shows means ± SEM.

We confirmed the role of the putative NLS in SH-SY5Y cells. This neuroblastoma-derived cell line can be differentiated to yield a neuron-like, non-proliferating phenotype using retinoic acid (Encinas et al., 2000). Consistent with the observations using HEK293T cells, differentiated SH-SY5Y cells showed a mixed nuclear/cytoplasmic distribution of RGNEF-wt, whereas cells expressing RGNEF-mutNLS had RGNEF mostly excluded from the nucleus (Fig. 3).

From the functional point of view, RGNEF carrying the mutated NLS was unable to activate RhoA in contrast RGNEF-wt in which RhoA activation was observed (Fig S2A and B). Additionally, RGNEF-mutNLS was unable to induce the formation of f-actin when overexpressed, in contrast to that observed with RGNEF-wt transfections (Fig S2C).

These results suggest that the PH domain of RGNEF contains a putative NLS and confirms that the 4 basic residues are critical to mediate nuclear localization and in addition, contribute directly to RGNEF's GEF activity.

### *3.3. The PH domain of RGNEF alone is sufficient to translocate a 160 kDa protein into the nucleus*

Having observed that the NLS was necessary for the nuclear localization of full length RGNEF, we next determined whether this domain alone was sufficient for the nuclear localization of a protein greater than 110 kDa, the maximum proposed threshold for passive diffusion of protein to the nucleus (Wang and Brattain, 2007). For this purpose, we utilized the pHM830 vector (Sorg and Stamminger, 1999) which adds an N-terminal green fluorescent protein (eGFP) and a C-terminal beta-galactosidase (LacZ) to the insert of interest in the multicloning site. Plasmids pHM830-PH-wt and pHM830-PH-mutNLS generated the 160 kDa fusion proteins: 830-PH-wt and 830-PH-mutNLS (Fig. 4A). When expressed in HEK293T cells (Fig. 4B), 830-PH-wt showed moderate levels of nuclear localization consistent with the observed with RGNEF-wt expression (Fig. 2B). Cells expressing the point-mutated form of the PH domain, 830-PH-mutNLS, showed a reduced amount of nuclear localization compared to 830-PH-wt, similar to the amount

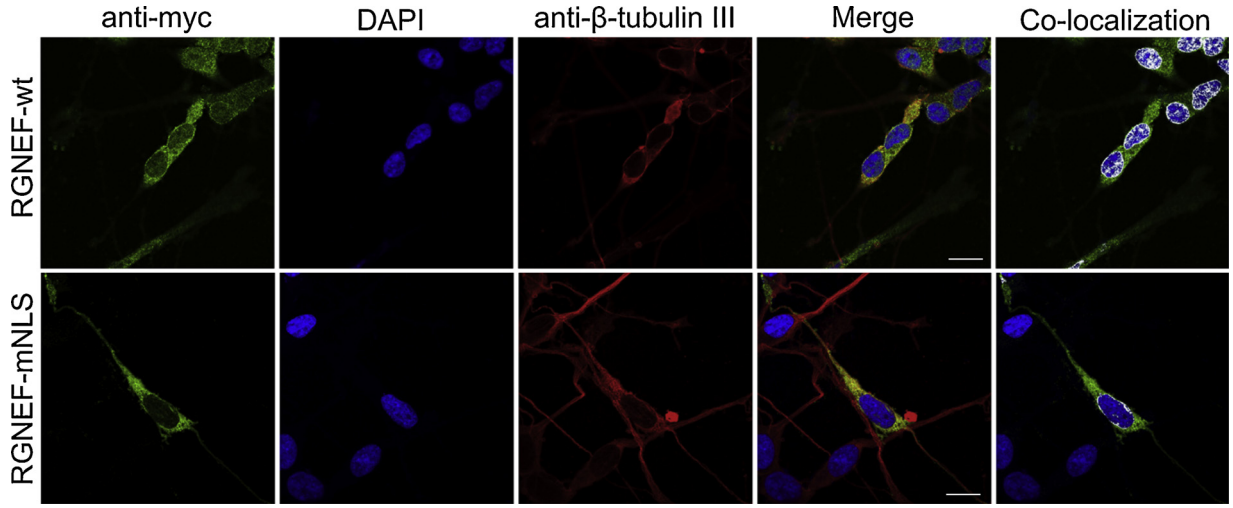


**Fig. 3.** RGNEF mutants lacking the NLS show lower levels of nuclear localization in a neuron-like cell type. Representative confocal images of differentiated SH-SY5Y cells transfected with myc-tagged RGNEF-wt or RGNEF-mutNLS. Cells were differentiating using 10 μM retinoic acid. β-Tubulin III was used as a marker of neuron-like phenotype to distinguish differentiated from non-differentiated cells. Moderate levels of nuclear localization were observed in cells transfected with RGNEF-wt, whereas cells transfected with either RGNEF-mutNLS do not. Scale bar = 15 μm.

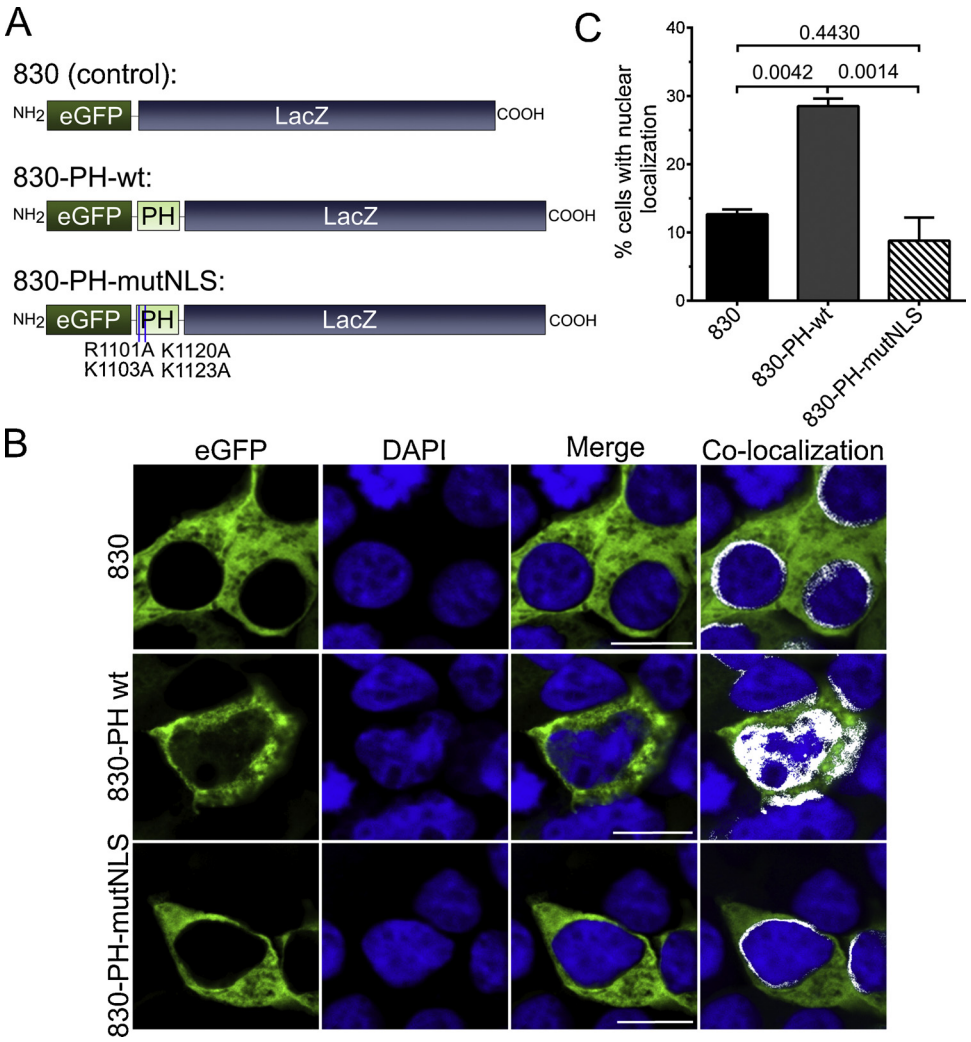


**Fig. 4.** Wild type, but not the mutated PH domain, is able to translocate a 160 kDa fusion protein to the nucleus. (A) Schematic representation of the pHM830 constructs used in this experiment. (B) Representative confocal images of HEK293 T cells transfected with empty pHM830 vector, pHM830 expressing the wild-type PH domain (830-PH-wt) or expressing the PH domain containing NLS mutations (830-PH-mutNLS). Scale bar = 15 μm. (C) Quantification of cellular localization of confocal images of the experiment showed in B. Cells transfected with pH830-PH-wt show a significantly higher percentage of nuclear localization compared to these transfected with either empty pHM830 vector or pH830-PHmNLS. Means were compared by ANOVA using Tukey's post-hoc test and p values are indicated. Graph shows means ± SEM.

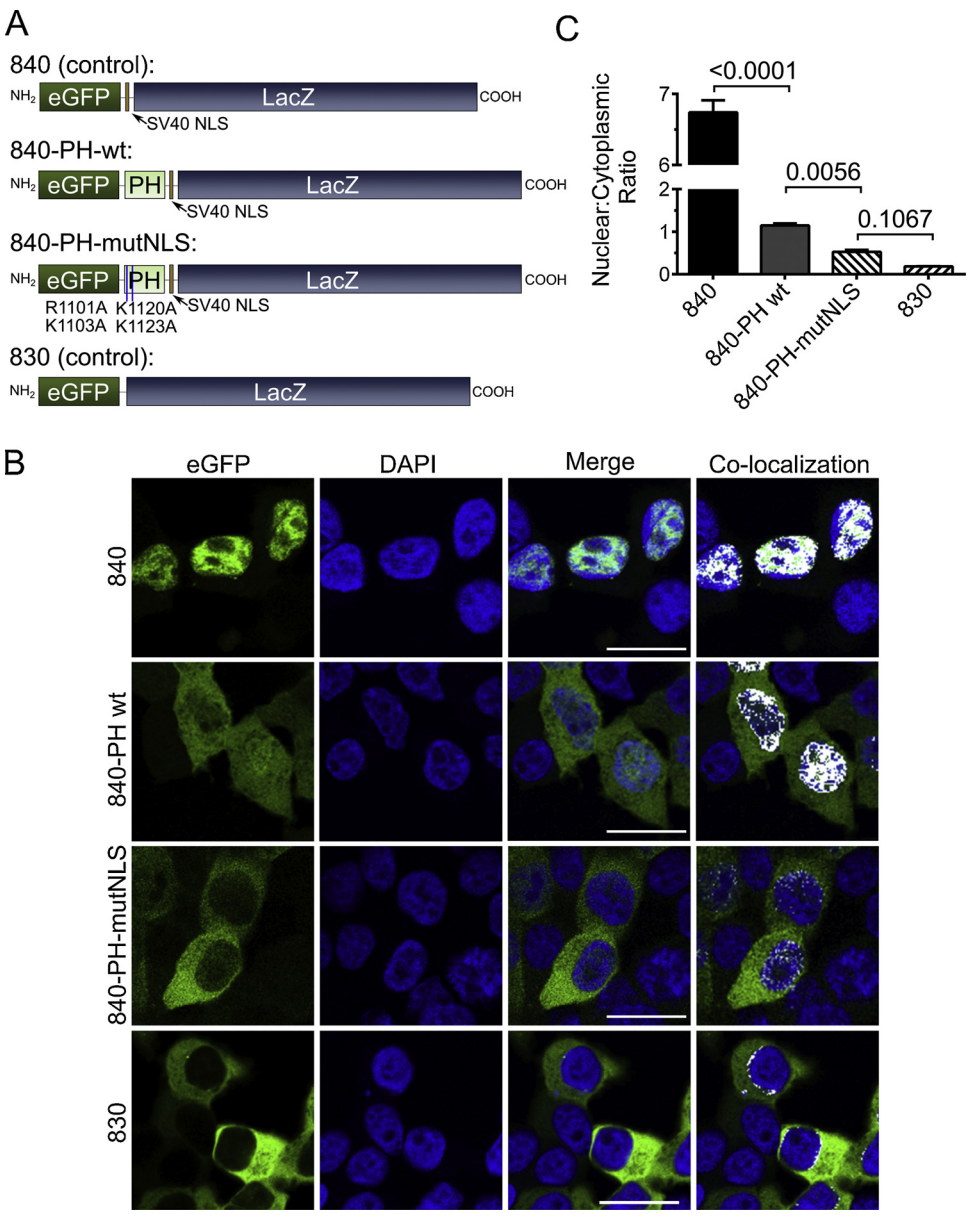


**Fig. 5.** The PH domain of RGNEF contains an active NES. (A) Schematic representation of the pH840 constructs used in this experiment. Note the presence of the SV40 NLS C-terminal to the PH domain insert (B) Representative confocal images of HEK293T cells transfected with empty pHM830 and pHM840 vectors, pHM840-PH-wt, and pHM840-PH-mutNLS. Scale bar = 15 µm. (C) Quantification of nuclear:cytoplasmic ratios generated from confocal images of HEK293T transfected with constructs showed in A. Cells transfected with empty pHM840 vector showed very high levels of nuclear localization, as expected given the NLS present in the vector. Cells transfected with the wild-type PH domain (840-PH-wt) showed lower levels of nuclear localization and those transfected with the mutated NLS PH domain (840-mutNLS) showed even lower levels. Means compared by ANOVA using Tukey's post-hoc test. Graph shows means ± SEM.

observed in cells transfected with pHM830 vector alone as control of cytoplasmic localization (Fig. 4B). Quantification of cells expressing the proteins found that a significantly higher percentage of cells containing 830-PHwt showed nuclear localization than either 830-PH-mutNLS ($p = 0.0014$) or control (empty vector) ($p = 0.0042$) (Fig. 4C). These results suggest that the presence of the PH domain is sufficient to translocate a protein greater than the largest passively diffusible size described (110 kDa) into the nucleus.

### 3.4. The PH domain-embedded NLS contains an overlapping NES

Interestingly, 830-PH-wt showed moderate levels of cytoplasmic localization, even though we would expect localization to be predominantly nuclear in an NLS containing protein. This suggested that the PH domain may also contains a NES. For this reason, we utilized the pHM840 vector (Sorg and Stamminger, 1999), which like the pHM830 vector encodes for the addition of both eGFP and LacZ, but also contains the SV40 NLS for nuclear localization (Fig. 5A). When expressed in HEK293 T cells, the protein encoded by the pHM840 vector alone localized almost exclusively to the nucleus as expected for a large, NLS containing protein (Fig. 5B). Quantified as nuclear:cytoplasmic ratio to obtain a measurement of the degree of translocation of the different constructs, nuclear localization was significantly decreased in cells expressing 840-PH-wt, suggesting that the PH domain contains a sequence sufficient to induce nuclear export despite the presence of the two NLS signals ($p < 0.0001$). Cells containing 840-PH-mutNLS showed even lower levels of nuclear localization than 840-PH-wt ($p = 0.0056$), consistent with what we would expect given that it contains the inactivated mutant NLS of the PH domain, but still having a functional SV40 NLS. As expected, the protein encoded by the PHM830 vector only shows cytoplasmic localization (Fig. 5C and Fig S1C). This data suggests the presence of an active NES in the PH domain of RGNEF and also support our previous finding that the wild-type PH contains an active NLS.

We then used in silico techniques to identify the location of the NES. The software NetNES 1.1 (la Cour et al., 2004) yielded NES scores above threshold for 9 residues of a 10 residue stretch within the linker region of the bipartite NLS, suggesting the presence of an NES within this region (Fig S3A). Alignment against the amino acid sequences of nine other NES previously identified in the literature (Kutay and Guttinger, 2005) found conserved identity among the hydrophobic residues of the traditional consensus NES motif $\Phi 1X_{(2,3)}\Phi 2X_{(2,3)}\Phi 3X\Phi 4$

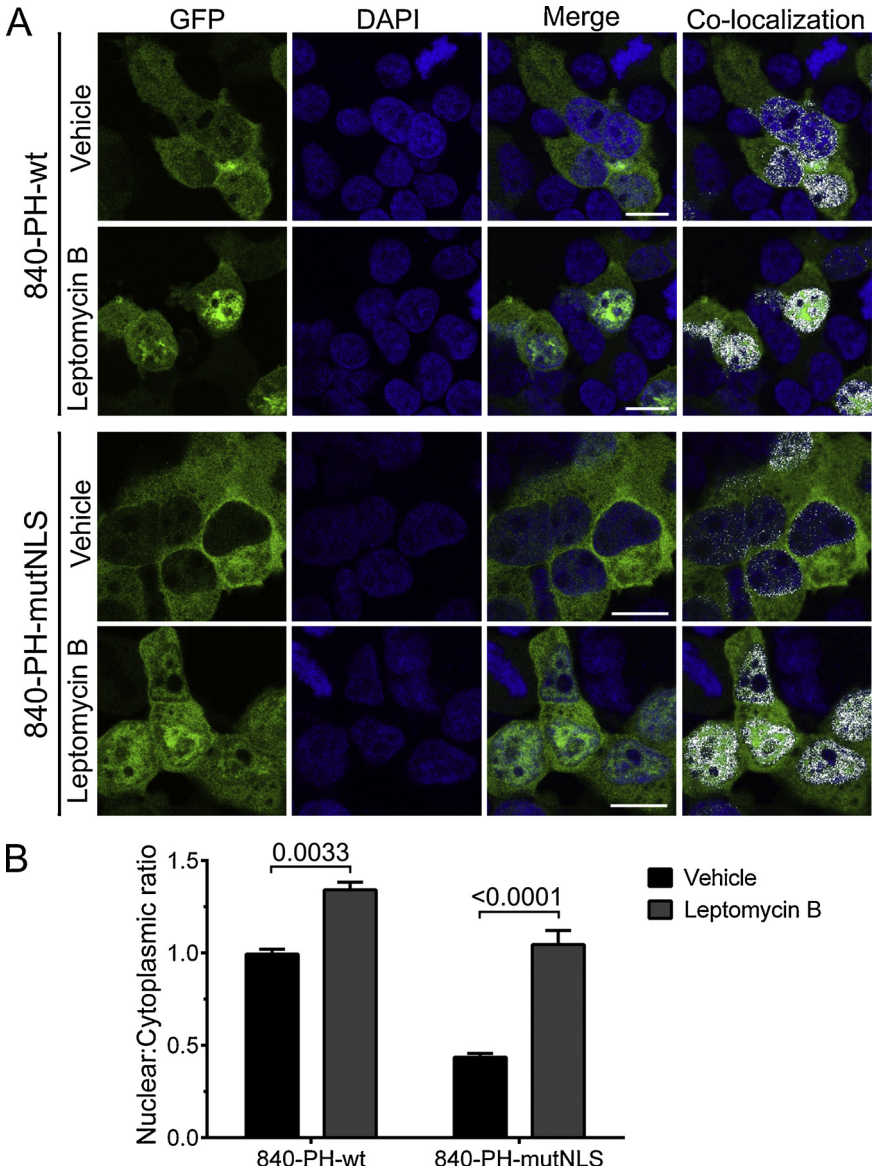


**Fig. 6.** The nuclear export of fusion proteins containing the PH domain of RGNEF depends of exportin-1. (A) Representative confocal images of HEK293T cells expressing 840-PH-wt and 840-PH-mutNLS and treated with either Leptomycin-B (LMB) or ethanol (vehicle). Scale bar = 15 μm. (B) nuclear:cytoplasmic ratios generated for HEK293T cells transfected with either of the two pHM840 constructs and treated with either 20 nM LMB or equal volume of ethanol (vehicle). Means were compared by ANOVA using Tukey's post-hoc test. Graph shows means ± SEM.

(Φn = L, V, I, F, or M) (Bogerd et al., 1996) within this region (Fig S3B). Comparison of this region with the six subclasses of NES sequences (Kosugi et al., 2008b) showed that, because of the high concentration of hydrophobic residues, this region can constitute any of the six subclasses of NES described (Fig S3C). Molecular modeling of the PH domain shows that, although when observed as a linear amino acid sequence the NES lies within the NLS, when depicted as a molecular model the residues of the NLS and NES are in close proximity but independent of one another (Fig S3D).

### 3.5. Nuclear export of the PH domain is exportin-1 dependent

To confirm the presence of a classical NES embedded within the PH domain, we treated HEK293 T cells with Leptomycin-B (LMB) for 4 h, 20 h after the transfection with either of the two pHM840 constructs expressing 840-PH-wt or 840-PH-mutNLS. LMB specifically blocks NES-dependent nuclear export by covalently binding exportin-1 (Kudo et al., 1999). Cells expressing either construct of the PH domain showed significantly higher levels of nuclear localization (840-PH-wt, $p = 0.0033$; 840-PH-mutNLS, $p < 0.0001$) when treated with LMB than when treated with vehicle (Fig. 6A and B), suggesting that this region does function as a NES, and that it functions in an exportin-1-dependent manner.

## 4. Discussion

In this study we have identified for the first time a single overlapping NLS/NES pair embedded within the PH domain of RGNEF. Previous observations by our group have described the presence of RGNEF in the nucleus (Droppelmann et al., 2013). Here, we demonstrated that in the absence of the PH domain, RGNEF localizes exclusively to the cytoplasm. Using *in silico* analysis, we identified a bipartite NLS within a 23-amino acid region of this PH domain. We created a series of constructs containing the PH domain with a mutated NLS and observed that, in contrast to the intact NLS signal which allowed for translocation, these mutated constructs were unable to

translocate to the nucleus. Additionally, we identified the presence of an NES within the PH domain that was analyzed using the pHM840 constructs containing the SV40 NLS. The nuclear localization of the 840 fusion proteins containing the PH-wt domain and the PH-mutNLS domain were observed to be reduced compared to the control. The NES function was determined to be exportin-1 dependent after Leptomycin-B treatment, which was sufficient to retain the constructs in the nucleus. Our analysis also showed for the first time an NES that is embedded within the linker region of the NLS. It worth noting that the difference in the nuclear:cytoplasmic ratio between the 840-PH-wt and 840-PH-mutNLS proteins is an indirect indication of the strength of the RGNEF NLS since the reduction observed in this ratio when the RGNEF NLS is mutated (but the SV40 NLS is still active) suggests how much the RGNEF NLS was pulling the protein into the nucleus.

In regards to other PH domains, an NLS has been found embedded within the intervening region of the Split Pleckstrin Homology (sPH) domain of Phosphoinositol 3-Kinase Enhancer (PIKE) (Yan et al., 2008). sPH domains are similar to PH domains in that they share the same molecular folding and localize proteins to membranes but are characterized by an intervening region within the seven-stranded anti-parallel β-sandwich (Wen et al., 2006; Yan et al., 2005). The sPH domain-embedded NLS is not only necessary for nuclear localization but also increases the sPH domain's affinity to localize to the membrane (Yan et al., 2008).

Given that the canonical role of PH domains is to bind phosphoinositides using basic residues, and that NLSs use basic residues to bind importin-α, it is reasonable to believe that these two functional domains would overlap more often than what is reported in the literature. For instance, two of the basic residues of the NLS identified here were previously described to be necessary for localization of RGNEF to the plasma membrane (Miller et al., 2014, 2013). This implies that those amino acids could be critical for RGNEF's GEF activity, as suggested by Schlaepfer's et al., through an auto-inhibitory mechanism of the PH domain over the DH domain which is released when RGNEF binds the membrane (Miller et al., 2014). This hypothesis could explain our findings regarding the inability of RGNEF-mutNLS to activate RhoA and to induce the formation of f-actin, in contrast to that observed with RGNEF-wt (Fig S2).

We gathered the amino acid sequences for 17 proteins containing PH domains and analyzed their respective sequences using cNLS Mapper (Table S1). Seven of the PH domains analyzed had a score equal or higher to what was found in RGNEF (Table S1- Highlighted cNLS Mapper scores). From that group, three proteins analyzed have a molecular weight greater than the 60 kDa threshold for nuclear diffusion (Fontes et al., 2000; Gorlich and Mattaj, 1996; Mattaj and Englmeier, 1998) and have been found to show localization into the nucleus (Table S1 – Highlighted molecular weights). From those three proteins we modeled the PDK1 protein because it had the highest score on cNLS mapper. Similar to what was found with the PH domain of RGNEF, the basic residues of the putative NLS were located on the exterior of the domain (Fig S3E), suggesting that they could be available for interaction with importin-α. Although the mechanism for nuclear localization of PDK1 has yet to be identified (Lim et al., 2003), a PH domain-embedded NLS has been also predicted using ProDom in its Drosophila homologue, known as Dstpk61 (Clyde and Bownes, 2000).

There are reports of a NES and NLS being located in close proximity or with some degree of overlap. For example, the NLS and NES of Heterogenous Nuclear Ribonucleoprotien A1 (hnRNP A1) are both located within the 38 residue M9 domain (Michael et al., 1995; Pollard et al., 1996; Siomi and Dreyfuss, 1995; Weighardt et al., 1995). As well, the NES and NLS of Transporter Associated with Antigen Processing (TAP) have been described as partially overlapping (Bear et al., 1999) and in the case of the yeast protein Pan1, have been described as an overlapping NES with its NLS number 3 although the NLS is not functional unless the NES is inactivated (Kaminska et al., 2007). In the PH domain of RGNEF, our data clearly show that when represented as a linear amino acid sequence, the NES lies completely within the linker region of the NLS and both are functional. When folded, the NLS and NES are close in proximity but are independent of one another (Fig S3D), suggesting no accessibility interference between both signals.

A growing body of work exists in the literature implicating nucleocytoplasmic transport dysfunction as a pathological component of ALS (See (Jovicic et al., 2016; Kim and Taylor, 2017) for reviews). Mutations in chromosome 9 open reading frame 72 (*C9orf72)*, observed in approximately 40% of all fALS cases (Renton et al., 2014), have been implicated in dysfunction of the nuclear import pathway across a range of species (Boeynaems et al., 2016; Jovicic et al., 2015; Kwon et al., 2014). Additionally, TDP-43, a major component of the neuronal cytoplasmic inclusions observed in ALS (Arai et al., 2006; Neumann et al., 2006), has been observed to have a pathological cytoplasmic localization when its nuclear import is altered (Winton et al., 2008). At the same time, it has been demonstrated that pathological cytoplasmic distributed TDP-43 disrupts the nucleocytoplasmic transport of nucleoporins and transport factors (Chou et al., 2018). This evidence suggests that alterations of normal nuclear-cytoplasm shuttling of RGNEF could have a negative impact on RGNEF functionality due to the formation of cytoplasmic inclusions that sequester RGNEF from its normal function.

In summary, here we have identified for the first time a PH domain containing an overlapping NLS/NES pair. We have shown that the PH domain is sufficient for both the nuclear import and export of RGNEF and, considering the analysis of other PH domain-containing proteins, we suggest the possibility that PH domain embedded NLSs may be more common than currently reported in the literature.

## Declaration of interest

The authors declare that they have no competing interests.

## Acknowledgments

This work was supported by the McFeat Family Fund, the Michael Halls Foundation, and the ALS Society of Canada.

## Appendix A. Supplementary data

Supplementary material related to this article can be found, in the online version, at doi:https://doi.org/10.1016/j.ejcb.2018.11.001.

## References

Arai, T., Hasegawa, M., Akiyama, H., Ikeda, K., Nonaka, T., Mori, H., Mann, D., Tsuchiya, K., Yoshida, M., Hashizume, Y., Oda, T., 2006. TDP-43 is a component of ubiquitin-positive tau-negative inclusions in frontotemporal lobar degeneration and amyotrophic lateral sclerosis. Biochem. Biophys. Res. Commun. 351, 602–611.

Bear, J., Tan, W., Zolotukhin, A.S., Tabernero, C., Hudson, E.A., Felber, B.K., 1999. Identification of novel import and export signals of human TAP, the protein that binds to the constitutive transport element of the type D retrovirus mRNAs. Mol. Cell. Biol. 19, 6306–6317.

Bertagnolo, V., Marchisio, M., Volinia, S., Caramelli, E., Capitani, S., 1998. Nuclear association of tyrosine-phosphorylated Vav to phospholipase C-gamma1 and phosphoinositide 3-kinase during granulocytic differentiation of HL-60 cells. FEBS Lett. 441, 480–484.

Boeynaems, S., Bogaert, E., Michiels, E., Gijselinck, I., Sieben, A., Jovicic, A., De Baets, G., Scheveneels, W., Steyaert, J., Cuijt, I., Verstrepen, K.J., Callaerts, P., Rousseau, F., Schymkowitz, J., Cruts, M., Van Broeckhoven, C., Van Damme, P., Gitler, A.D., Robberecht, W., Van Den Bosch, L., 2016. Drosophila screen connects nuclear transport genes to DPR pathology in c9ALS/FTD. Sci. Rep. 6, 20877.

Bogerd, H.P., Fridell, R.A., Benson, R.E., Hua, J., Cullen, B.R., 1996. Protein sequence requirements for function of the human T-cell leukemia virus type 1 Rex nuclear export signal delineated by a novel in vivo randomization-selection assay. Mol. Cell. Biol. 16, 4207–4214.

Cheung, K., Droppelmann, C.A., MacLellan, A., Cameron, I., Withers, B., Campos-Melo, D., Volkening, K., Strong, M.J., 2017. Rho guanine nucleotide exchange factor (RGNEF) is a prosurvival factor under stress conditions. Mol. Cell. Neurosci. 82, 88–95.

Chou, C.C., Zhang, Y., Umoh, M.E., Vaughan, S.W., Lorenzini, I., Liu, F., Sayegh, M., Donlin-Asp, P.G., Chen, Y.H., Duong, D.M., Seyfried, N.T., Powers, M.A., Kukar, T., Hales, C.M., Gearing, M., Cairns, N.J., Boylan, K.B., Dickson, D.W., Rademakers, R.,

Zhang, Y.J., Petrucelli, L., Sattler, R., Zarnescu, D.C., Glass, J.D., Rossoll, W., 2018. TDP-43 pathology disrupts nuclear pore complexes and nucleocytoplasmic transport in ALS/FTD. Nat. Neurosci. 21, 228–239.
Clyde, D., Bownes, M., 2000. The Dstpk61 locus of Drosophila produces multiple transcripts and protein isoforms, suggesting it is involved in multiple signalling pathways. J. Endocrinol. 167, 391–401.
Cozier, G.E., Carlton, J., Bouyoucef, D., Cullen, P.J., 2004. Membrane targeting by pleckstrin homology domains. Curr. Top. Microbiol. Immunol. 282, 49–88.
Dingwall, C., Laskey, R.A., 1991. Nuclear targeting sequences–a consensus? Trends Biochem. Sci. 16, 478–481.
Droppelmann, C.A., Keller, B.A., Campos-Melo, D., Volkening, K., Strong, M.J., 2013. Rho guanine nucleotide exchange factor is an NFL mRNA destabilizing factor that forms cytoplasmic inclusions in amyotrophic lateral sclerosis. Neurobiol. Aging 34, 248–262.
Droppelmann, C.A., Campos-Melo, D., Volkening, K., Strong, M.J., 2014. The emerging role of guanine nucleotide exchange factors in ALS and other neurodegenerative diseases. Front. Cell. Neurosci. 8, 282.
Encinas, M., Iglesias, M., Liu, Y., Wang, H., Muhaisen, A., Cena, V., Gallego, C., Comella, J.X., 2000. Sequential treatment of SH-SY5Y cells with retinoic acid and brain-derived neurotrophic factor gives rise to fully differentiated, neurotrophic factor-dependent, human neuron-like cells. J. Neurochem. 75, 991–1003.
Fontes, M.R., Teh, T., Kobe, B., 2000. Structural basis of recognition of monopartite and bipartite nuclear localization sequences by mammalian importin-alpha. J. Mol. Biol. 297, 1183–1194.
Gorlich, D., Mattaj, I.W., 1996. Nucleocytoplasmic transport. Science 271, 1513–1518.
Henderson, B.R., Eleftheriou, A., 2000. A comparison of the activity, sequence specificity, and CRM1-dependence of different nuclear export signals. Exp. Cell Res. 256, 213–224.
Hubner, S., Xiao, C.Y., Jans, D.A., 1997. The protein kinase CK2 site (Ser111/112) enhances recognition of the simian virus 40 large T-antigen nuclear localization sequence by importin. J. Biol. Chem. 272, 17191–17195.
Jovicic, A., Mertens, J., Boeynaems, S., Bogaert, E., Chai, N., Yamada, S.B., Paul 3rd, J.W., Sun, S., Herdy, J.R., Bieri, G., Kramer, N.J., Gage, F.H., Van Den Bosch, L., Robberecht, W., Gitler, A.D., 2015. Modifiers of C9orf72 dipeptide repeat toxicity connect nucleocytoplasmic transport defects to FTD/ALS. Nat. Neurosci. 18, 1226–1229.
Jovicic, A., Paul 3rd, J.W., Gitler, A.D., 2016. Nuclear transport dysfunction: a common theme in amyotrophic lateral sclerosis and frontotemporal dementia. J. Neurochem. 138 (Suppl 1), 134–144.
Kalderon, D., Richardson, W.D., Markham, A.F., Smith, A.E., 1984a. Sequence requirements for nuclear location of simian virus 40 large-T antigen. Nature 311, 33–38.
Kalderon, D., Roberts, B.L., Richardson, W.D., Smith, A.E., 1984b. A short amino acid sequence able to specify nuclear location. Cell 39, 499–509.
Kaminska, J., Sedek, M., Wysocka-Kapcinska, M., Zoladek, T., 2007. Characterization of nuclear localization and nuclear export signals of yeast actin-binding protein Pan1. FEBS Lett. 581, 5371–5376.
Keller, B.A., Volkening, K., Droppelmann, C.A., Ang, L.C., Rademakers, R., Strong, M.J., 2012. Co-aggregation of RNA binding proteins in ALS spinal motor neurons: evidence of a common pathogenic mechanism. Acta Neuropathol. 124, 733–747.
Kim, H.J., Taylor, J.P., 2017. Lost in Transportation: Nucleocytoplasmic Transport Defects in ALS and Other Neurodegenerative Diseases. Neuron 96, 285–297.
Kim, C.G., Park, D., Rhee, S.G., 1996. The role of carboxyl-terminal basic amino acids in Gqalpha-dependent activation, particulate association, and nuclear localization of phospholipase C-beta1. J. Biol. Chem. 271, 21187–21192.
Kosugi, S., Hasebe, M., Entani, T., Takayama, S., Tomita, M., Yanagawa, H., 2008a. Design of peptide inhibitors for the importin alpha/beta nuclear import pathway by activity-based profiling. Chem. Biol. 15, 940–949.
Kosugi, S., Hasebe, M., Tomita, M., Yanagawa, H., 2008b. Nuclear export signal consensus sequences defined using a localization-based yeast selection system. Traffic 9, 2053–2062.
Kosugi, S., Hasebe, M., Matsumura, N., Takashima, H., Miyamoto-Sato, E., Tomita, M., Yanagawa, H., 2009a. Six classes of nuclear localization signals specific to different binding grooves of importin alpha. J. Biol. Chem. 284, 478–485.
Kosugi, S., Hasebe, M., Tomita, M., Yanagawa, H., 2009b. Systematic identification of cell cycle-dependent yeast nucleocytoplasmic shuttling proteins by prediction of composite motifs. Proc Natl Acad Sci U S A 106, 10171–10176.
Kudo, N., Matsumori, N., Taoka, H., Fujiwara, D., Schreiner, E.P., Wolff, B., Yoshida, M., Horinouchi, S., 1999. Leptomycin B inactivates CRM1/exportin 1 by covalent modification at a cysteine residue in the central conserved region. Proc Natl Acad Sci U S A 96, 9112–9117.
Kutay, U., Guttinger, S., 2005. Leucine-rich nuclear-export signals: born to be weak. Trends Cell Biol. 15, 121–124.
Kwon, I., Xiang, S., Kato, M., Wu, L., Theodoropoulos, P., Wang, T., Kim, J., Yun, J., Xie, Y., McKnight, S.L., 2014. Poly-dipeptides encoded by the C9orf72 repeats bind nucleoli, impede RNA biogenesis, and kill cells. Science 345, 1139–1145.
la Cour, T., Kiemer, L., Molgaard, A., Gupta, R., Skriver, K., Brunak, S., 2004. Analysis and prediction of leucine-rich nuclear export signals. Protein Eng. Des. Sel. 17, 527–536.
Lange, A., Mills, R.E., Lange, C.J., Stewart, M., Devine, S.E., Corbett, A.H., 2007. Classical nuclear localization signals: definition, function, and interaction with importin alpha. J. Biol. Chem. 282, 5101–5105.
Lange, A., McLane, L.M., Mills, R.E., Devine, S.E., Corbett, A.H., 2010. Expanding the definition of the classical bipartite nuclear localization signal. Traffic 11, 311–323.
Lemmon, M.A., 2004. Pleckstrin homology domains: not just for phosphoinositides. Biochem. Soc. Trans. 32, 707–711.
Lemmon, M.A., Ferguson, K.M., 2000. Signal-dependent membrane targeting by pleckstrin homology (PH) domains. Biochem. J. 350 (Pt 1), 1–18.
Lim, M.A., Kikani, C.K., Wick, M.J., Dong, L.Q., 2003. Nuclear translocation of 3'-phosphoinositide-dependent protein kinase 1 (PDK-1): a potential regulatory mechanism for PDK-1 function. Proc Natl Acad Sci U S A 100, 14006–14011.
Liu, X., Fagotto, F., 2011. A method to separate nuclear, cytosolic, and membrane-associated signaling molecules in cultured cells. Sci. Signal. 4, pl2.
Marfori, M., Mynott, A., Ellis, J.J., Mehdi, A.M., Saunders, N.F., Curmi, P.M., Forwood, J.K., Boden, M., Kobe, B., 2011. Molecular basis for specificity of nuclear import and prediction of nuclear localization. Biochim. Biophys. Acta 1813, 1562–1577.
Marmiroli, S., Ognibene, A., Bavelloni, A., Cinti, C., Cocco, L., Maraldi, N.M., 1994. Interleukin 1 alpha stimulates nuclear phospholipase C in human osteosarcoma SaOS-2 cells. J. Biol. Chem. 269, 13–16.
Mattaj, I.W., Englmeier, L., 1998. Nucleocytoplasmic transport: the soluble phase. Annu. Rev. Biochem. 67, 265–306.
Michael, W.M., Choi, M., Dreyfuss, G., 1995. A nuclear export signal in hnRNP A1: a signal-mediated, temperature-dependent nuclear protein export pathway. Cell 83, 415–422.
Miller, N.L., Lawson, C., Kleinschmidt, E.G., Tancioni, I., Uryu, S., Schlaepfer, D.D., 2013. A non-canonical role for Rgnef in promoting integrin-stimulated focal adhesion kinase activation. J. Cell. Sci. 126, 5074–5085.
Miller, N.L., Kleinschmidt, E.G., Schlaepfer, D.D., 2014. RhoGEFs in cell motility: novel links between Rgnef and focal adhesion kinase. Curr. Mol. Med. 14, 221–234.
Neumann, M., Sampathu, D.M., Kwong, L.K., Truax, A.C., Micsenyi, M.C., Chou, T.T., Bruce, J., Schuck, T., Grossman, M., Clark, C.M., McCluskey, L.F., Miller, B.L., Masliah, E., Mackenzie, I.R., Feldman, H., Feiden, W., Kretzschmar, H.A., Trojanowski, J.Q., Lee, V.M., 2006. Ubiquitinated TDP-43 in frontotemporal lobar degeneration and amyotrophic lateral sclerosis. Science 314, 130–133.
Nore, B.F., Vargas, L., Mohamed, A.J., Branden, L.J., Backesjo, C.M., Islam, T.C., Mattsson, P.T., Hultenby, K., Christensson, B., Smith, C.I., 2000. Redistribution of Bruton's tyrosine kinase by activation of phosphatidylinositol 3-kinase and Rho-family GTPases. Eur. J. Immunol. 30, 145–154.
Peters, R., 1984. Nucleo-cytoplasmic flux and intracellular mobility in single hepatocytes measured by fluorescence microphotolysis. EMBO J. 3, 1831–1836.
Pollard, V.W., Michael, W.M., Nakielny, S., Siomi, M.C., Wang, F., Dreyfuss, G., 1996. A novel receptor-mediated nuclear protein import pathway. Cell 86, 985–994.
Pountney, D.L., Raftery, M.J., Chegini, F., Blumbergs, P.C., Gai, W.P., 2008. NSF, Unc-18-1, dynamin-1 and HSP90 are inclusion body components in neuronal intranuclear inclusion disease identified by anti-SUMO-1-immunocapture. Acta Neuropathol. 116, 603–614.
Renton, A.E., Chio, A., Traynor, B.J., 2014. State of play in amyotrophic lateral sclerosis genetics. Nat. Neurosci. 17, 17–23.
Roy, A., Kucukural, A., Zhang, Y., 2010. I-TASSER: a unified platform for automated protein structure and function prediction. Nat. Protoc. 5, 725–738.
Siomi, H., Dreyfuss, G., 1995. A nuclear localization domain in the hnRNP A1 protein. J. Cell Biol. 129, 551–560.
Sorg, G., Stamminger, T., 1999. Mapping of nuclear localization signals by simultaneous fusion to green fluorescent protein and to beta-galactosidase. Biotechniques 26, 858–862.
Stallings, J.D., Tall, E.G., Pentyala, S., Rebecchi, M.J., 2005. Nuclear translocation of phospholipase C-delta1 is linked to the cell cycle and nuclear phosphatidylinositol 4,5-bisphosphate. J. Biol. Chem. 280, 22060–22069.
Tang, Y., Katuri, V., Dillner, A., Mishra, B., Deng, C.X., Mishra, L., 2003. Disruption of transforming growth factor-beta signaling in ELF beta-spectrin-deficient mice. Science 299, 574–577.
Volkening, K., Leystra-Lantz, C., Strong, M.J., 2010. Human low molecular weight neurofilament (NFL) mRNA interacts with a predicted p190RhoGEF homologue (RGNEF) in humans. Amyotroph. Lateral Scler. 11, 97–103.
Wang, R., Brattain, M.G., 2007. The maximal size of protein to diffuse through the nuclear pore is larger than 60kDa. FEBS Lett. 581, 3164–3170.
Weighardt, F., Biamonti, G., Riva, S., 1995. Nucleo-cytoplasmic distribution of human hnRNP proteins: a search for the targeting domains in hnRNP A1. J. Cell. Sci. 108 (Pt 2), 545–555.
Wen, W., Yan, J., Zhang, M., 2006. Structural characterization of the split pleckstrin homology domain in phospholipase C-gamma1 and its interaction with TRPC3. J. Biol. Chem. 281, 12060–12068.
Winton, M.J., Igaz, L.M., Wong, M.M., Kwong, L.K., Trojanowski, J.Q., Lee, V.M., 2008. Disturbance of nuclear and cytoplasmic TAR DNA-binding protein (TDP-43) induces disease-like redistribution, sequestration, and aggregate formation. J. Biol. Chem. 283, 13302–13309.
Wu, J., 2003. Cytoplasmic retention sites in p190RhoGEF confer anti-apoptotic activity to an EGFP-tagged protein. Mol. Brain Res. 117, 27–38.
Xu, D., Farmer, A., Collett, G., Grishin, N.V., Chook, Y.M., 2012. Sequence and structural analyses of nuclear export signals in the NESdb database. Mol. Biol. Cell 23, 3677–3693.
Yamaga, M., Fujii, M., Kamata, H., Hirata, H., Yagisawa, H., 1999. Phospholipase C-delta1 contains a functional nuclear export signal sequence. J. Biol. Chem. 274, 28537–28541.
Yan, J., Wen, W., Xu, W., Long, J.F., Adams, M.E., Froehner, S.C., Zhang, M., 2005. Structure of the split PH domain and distinct lipid-binding properties of the PH-PDZ supramodule of alpha-syntrophin. EMBO J. 24, 3985–3995.
Yan, J., Wen, W., Chan, L.N., Zhang, M., 2008. Split pleckstrin homology domain-mediated cytoplasmic-nuclear localization of PI3-kinase enhancer GTPase. J. Mol. Biol. 378, 425–435.
Yang, J., Yan, R., Roy, A., Xu, D., Poisson, J., Zhang, Y., 2015. The I-TASSER Suite: protein structure and function prediction. Nat. Methods 12, 7–8.
Ye, K., Aghdasi, B., Luo, H.R., Moriarity, J.L., Wu, F.Y., Hong, J.J., Hurt, K.J., Bae, S.S., Suh, P.G., Snyder, S.H., 2002. Phospholipase C gamma 1 is a physiological guanine nucleotide exchange factor for the nuclear GTPase PIKE. Nature 415, 541–544.
Yu, H.G., Nam, J.O., Miller, N.L., Tanjoni, I., Walsh, C., Shi, L., Kim, L., Chen, X.L., Tomar, A., Lim, S.T., Schlaepfer, D.D., 2011. p190RhoGEF (Rgnef) promotes colon carcinoma tumor progression via interaction with focal adhesion kinase. Cancer Res. 71, 360–370.
Zhang, Y., 2008. I-TASSER server for protein 3D structure prediction. BMC Bioinformatics 9, 40.